

See discussions, stats, and author profiles for this publication at: <https://www.researchgate.net/publication/249995874>

Influence of Drug Encapsulation Within Mixed Micelles on the Excited State Dynamics and Accessibility to Ionic Quenchers.

ARTICLE *in* THE JOURNAL OF PHYSICAL CHEMISTRY B · JULY 2013

Impact Factor: 3.3 · DOI: 10.1021/jp404353u · Source: PubMed

CITATIONS

4

READS

43

5 AUTHORS, INCLUDING:



Inmaculada Andreu

IIS-Hospital Universitari i Politècnic la Fe

50 PUBLICATIONS 468 CITATIONS

SEE PROFILE



Miguel Angel Miranda

Universitat Politècnica de València

504 PUBLICATIONS 7,116 CITATIONS

SEE PROFILE

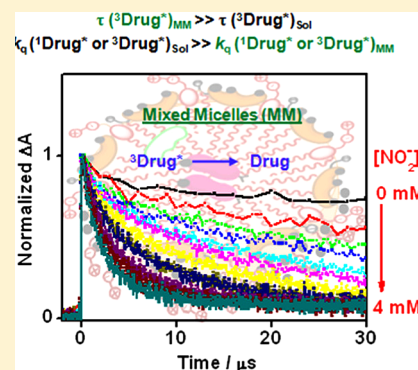
Influence of Drug Encapsulation within Mixed Micelles on the Excited State Dynamics and Accessibility to Ionic Quenchers

Eduar Nuin,[†] Miguel Gomez-Mendoza,[†] M. Luisa Marin,[†] Inmaculada Andreu,[‡] and Miguel A. Miranda^{*,†}

[†]Instituto Universitario Mixto de Tecnología Química (UPV-CSIC), Universitat Politècnica de València, Avenida de los Naranjos s/n, 46022 Valencia, Spain

[‡]Unidad Mixta de Investigación IIS La Fe–UPV, Hospital La Fe, Avda. Campanar 21, 46009 Valencia, Spain

ABSTRACT: Photophysical techniques, specifically time-resolved fluorescence and laser flash photolysis, have proven to be noninvasive, straightforward, and valuable tools to demonstrate how drug encapsulation into biomimetic mixed micelles (MM) influences the dynamics of excited states and their accessibility to ionic quenchers. This concept has been illustrated by choosing a set of currently administered drugs containing a common naphthalene chromophore, namely, (S)-naproxen and its methyl ester, (R)-cinacalcet and (S)-propranolol. A remarkable increase of their triplet lifetimes is noticed when experiments are performed in MM, indicating efficient entrapment of the drugs in these supramolecular entities. Furthermore, a decrease of 1 order of magnitude in the quenching rate constant of the singlet and triplet excited states (by iodide or nitrite, respectively) is observed upon encapsulation into MM. This approach can in principle be extended to other microenvironments capable of incorporating photoactive compounds.



INTRODUCTION

Encapsulation within biomimetic microenvironments, such as liposomes, cyclodextrins, micelles, or bile salts is a very versatile tool in biology, biochemistry, and medicine. These microheterogeneous systems have been employed as models to study the photochemical behavior of a variety of drugs and its dependence on the nature of the media.^{1–4}

In this context, mixed micelles (MM) made of phospholipids and bile salts have attracted increasing attention as nanocarriers in pharmaceutical formulations due to their important advantages, such as enhanced stability and reduced toxicity.^{5–9}

In fact, MM have already been employed as suitable vehicles for poorly water-soluble drugs, such as diazepam,⁵ tetrazepam,¹⁰ clonazepam,¹¹ diclofenac,^{12,13} indometacin,¹⁴ nimodipine,¹⁵ silybin,¹⁶ and vitamin K.¹⁷ In this connection, based on their physiological compatibility and solubilizing capability, MM have been successfully used in the intravenous delivery of taxol.¹⁸

Encapsulation of bioactive compounds into microheterogeneous media has been demonstrated by different techniques that include dynamic light scattering,^{19,20} transmission electron microscopy,²¹ capillary electrophoresis,²² calorimetry,²³ small-angle X-ray scattering,²⁴ ultracentrifugation,²⁵ and nuclear magnetic resonance.²⁶ However, most of them are based on indirect measurements and do not inform on the accessibility of the drugs inside biomimetic microenvironments. Therefore, more sensitive and direct methodologies would be desirable to investigate this matter. Recently, we have made use of photophysical techniques, specifically time-resolved fluorescence and laser flash photolysis (LFP), to prove the

incorporation of compounds with different hydrophobicity into cholic acid (CA) aggregates.²⁷ Additionally, we have employed a photoactive dansyl-labeled cholesterol derivative to reveal efficient incorporation of cholesterol (Ch) into the MM, thus demonstrating the outstanding solubilizing capability of MM.²⁸

With this background, the aim of the present work is to evaluate how the incorporation into biomimetic MM nanocarriers influences the excited state dynamics and accessibility to ionic quenchers. To achieve this goal, a few currently administered drugs containing a common naphthalene chromophore, appropriate for fluorescence and LFP experiments, have been selected. They include (S)-naproxen (NPX), a known nonsteroidal anti-inflammatory drug, (R)-cinacalcet (CIN), used as calcimimetic agent, and (S)-propranolol (PPN), a sympatholytic nonselective β -blocker employed for the treatment of hypertension (Figure 1A). The MM were prepared from lecithin (L), Ch, and CA following our recently reported procedure.²⁸

EXPERIMENTAL METHODS

Chemicals. Lecithin, prepared from fresh egg yolk, Ch, NPX, PPN hydrochloride, and NaCl were purchased from Sigma–Aldrich (Steinheim, Germany) and used as received. The methyl ester NPXMe was synthesized as previously reported,²⁹ and CIN was obtained from commercial Mimpara

Received: May 2, 2013

Revised: June 28, 2013

Published: July 17, 2013

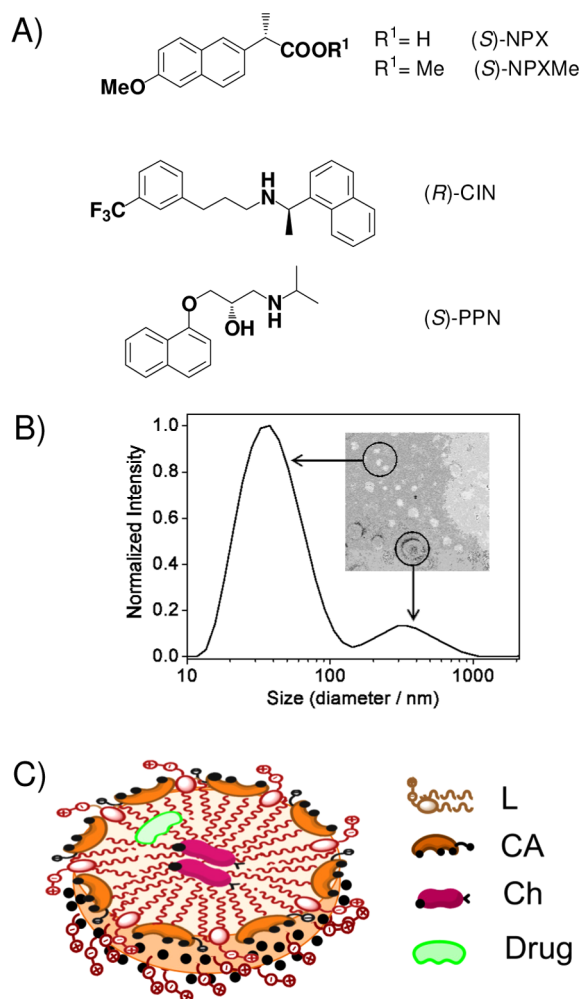


Figure 1. (A) Chemical structures of drugs NPX, CIN, PPN, and prodrug NPXMe. (B) DLS size distribution curves and TEM images for mixed micelles together with a small amount of vesicles in 0.2 M aqueous NaCl. (C) Cartoon representation of the drugs inside MM.

60 mg (Amgen, Spain). Thus, the content of six pills was powdered in a mortar, suspended in 1 M NH_4OH (150 mL), and extracted with CH_2Cl_2 (4×50 mL). The combined organic layers were washed with brine (3×150 mL) and water (3×150 mL), dried over MgSO_4 , and evaporated under reduced pressure. The residue was purified by column chromatography through silica gel 60 (dichloromethane/methanol/15 M ammonium hydroxide, 98:2:0.1 v/v/v) to give CIN as a colorless oil. Sodium cholate (NaCA) was provided by Acros Organics and used without further purification. All solvents used were of HPLC grade from Scharlab (Sentmenat, Spain). Milli-Q water was used for sample preparation.

Preparation of Mixed Micelles. To a solution of 17.8 μmol of L and 38.8 μmol of NaCA in methanol, Ch (5.4 μmol) and the appropriate amount of the drug (0.027 or 0.27 μmol for fluorescence or LFP experiments, respectively) dissolved in the minimum amount of CH_2Cl_2 were added. The combined solutions were concentrated for 30 min at 50 $^\circ\text{C}$, using a vacuum rotary evaporator, and then for 30 min at room temperature with an oil pump. The dry film obtained was hydrated with 1.37 mL of 0.2 M aqueous NaCl to form a clear MM solution.

Transmission Electron Microscopy (TEM). Images were collected with a Philips CM-10 microscope operating at 100 kV. A drop of the MM solution was sucked on a copper coated carbon grid for 1 min and then removed to leave a thin film. Then, negative staining was achieved using a drop of a 1% solution of ammonium molybdate for 1 min. After removal of the excess, the resulting stained film was allowed to dry in a dust-free place.

Dynamic Light Scattering (DLS). Size measurements were conducted on MM with a Zetasizer Nano ZS (Malvern Instruments Ltd., Worcestershire, United Kingdom). The prepared MM were diluted using deionized water and subjected to DLS measurements at 25 $^\circ\text{C}$ and 173 $^\circ$ scattering angles. The mean hydrodynamic diameter was obtained by cumulant analysis.

Photophysical Instrumentation. Steady-state fluorescence experiments were performed on a Photon Technology International (PTI, Germany) LPS-220B spectrofluorometer, equipped with a 75 W Xe lamp and a monochromator in the region of 200–700 nm. Time-resolved fluorescence measurements were carried out with a Time Master fluorescence lifetime spectrometer TM 2/2003 from PTI, equipped with a hydrogen/nitrogen flash lamp as the excitation source. Laser flash photolysis experiments were carried out with a pulsed Nd:YAG SL404G-10 Spectron Laser Systems ($\lambda_{\text{exc}} = 266$ nm, ca. 10 ns pulse width, <20 mJ per pulse). A pulsed Lo255 Oriel Xenon lamp was employed as detecting light source. The LFP equipment includes also a 77200 Oriel monochromator, an Oriel photomultiplier tube (PMT) system made up of a 77348 side-on PMT, 70680 PMT housing, a 70705 PMT power supply, and a TDS-640A Tektronix oscilloscope. The output signal from the oscilloscope was transferred to a personal computer.

Photophysical Experiments. Emission measurements were performed in the 330–600 nm region at 2×10^{-5} M concentration of the chromophore, under aerobic conditions. The kinetic traces were fitted by monoexponential decay functions, using a deconvolution procedure to separate them from the lamp pulse profile. For LFP experiments in 0.2 M NaCl aqueous solutions the samples were fixed by adjusting the absorbance of the solutions at the arbitrary value of 0.2 at excitation wavelength. When the LFP measurements were carried out in MM, the concentration of the chromophore was 2×10^{-4} M. The triplet lifetimes were obtained from the monoexponential fitting of the decay traces registered at 420 nm. All of the samples were bubbled with N_2 . The aqueous solutions, the films and the quartz cells were bubbled for 2 h, 1 h, and 30 min, respectively. All photophysical measurements were performed at room temperature using 10×10 mm² quartz cells with a 4 mL capacity.

RESULTS AND DISCUSSION

Formation of MM and encapsulation of the drugs was achieved in one pot. Thus, a combined dichloromethane solution of Ch and NPX, NPXMe, CIN, or PPN was added to a solution of L and CA in methanol. After evaporation of the solvent and subsequent rehydration of the film, MM containing the drugs were obtained. They were characterized by DLS and TEM measurements (Figure 1B); the results were similar to those obtained for MM containing dansyl derivatives as photoactive probes.²⁸ The cartoon represents a MM, in which NPX, NPXMe, CIN, or PPN have been incorporated into the hydrophobic part (Figure 1C).

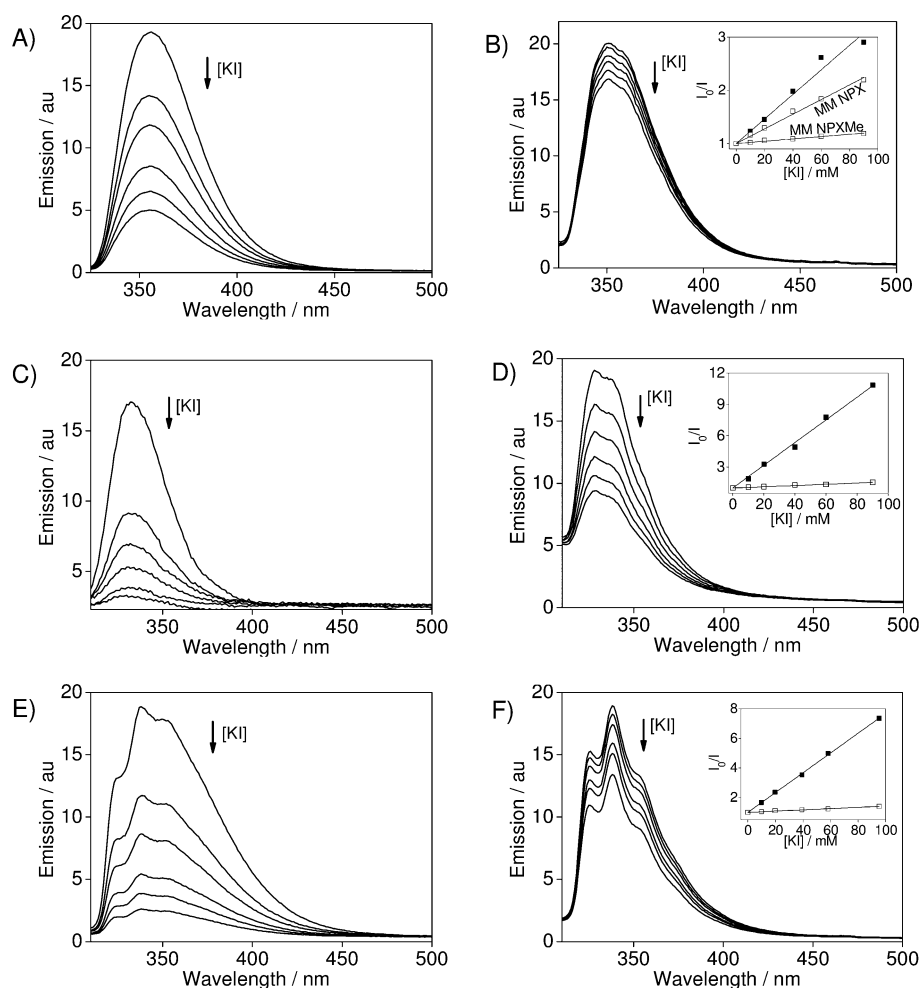


Figure 2. Emission spectra ($\lambda_{\text{exc}} = 290$ nm) upon addition of increasing amounts of KI (0–90 mM) of NPX in 0.2 M aqueous NaCl (A) and NPXMe into MM (B), CIN in 0.2 M aqueous NaCl (C) and into MM (D), and PPN in 0.2 M aqueous NaCl (E) and into MM (F). Insets: Stern–Volmer plots in solution (■) and in the presence of MM (□).

To check the influence of encapsulation inside MM on the drug excited states, fluorescence and LFP experiments were performed both in aqueous solution (except for the insoluble NPXMe) and in MM. First, the shape of UV–visible absorption spectra of the drugs was identical into MM and in solution. Upon excitation at 290 nm fluorescence emission spectra were observed in MM, with maxima at 356, 350, 332, and 338 nm for NPX, NPXMe, CIN, and PPN, respectively (Figure 2). In solution, the lifetimes of the singlet excited state were 8.3 ns (NPX), 28.6 ns (CIN), and 9.8 ns (PPN); no significant changes were observed between solution and MM, with the exception of PPN whose lifetime increased up to 14.3 ns. Steady-state and time-resolved quenching experiments with iodide, which mainly remains in water, were performed to assess the extent of encapsulation. Indeed, Figure 3 shows the dynamic nature of the NPXMe, CIN, and PPN quenching within MM upon addition of increasing concentrations of KI (in the range 0–90 mM).

In all cases, the corresponding Stern–Volmer analysis (eq 1) was compared to the results obtained in solution (see Figure 2 for steady-state measurements and Figure 3 for dynamic quenching).

$$I_0/I \text{ or } \tau_0/\tau = 1 + k_q\tau_0[I^-] \quad (1)$$

The quenching rate constant (k_q) values were determined from fluorescence lifetimes in solution ($k_{q,\text{sol}}$) and in MM ($k_{q,\text{MM}}$) upon addition of increasing quencher concentrations. Table 1 shows that the k_q of NPXMe, CIN, and PPN decreased by 1 order of magnitude when passing from solution to MM, whereas the k_q decrease observed for NPX was ca. one-half as an evidence of the different accessibility of the singlet excited states of the studied chromophores to iodide. It should be noticed that encapsulation of NPXMe, CIN, and PPN within MM was very efficient, since the slopes of the Stern–Volmer plots in solution and in MM were of different order of magnitude; however, in the case of NPX a less marked difference was observed, probably because of a different location of this drug into the MM, closer to the micelle surface.

These values are in complete accordance with the expectation based on the higher hydrophobicity of NPXMe, CIN, and PPN, compared to the free carboxylic acid NPX. Therefore, the fluorescence quenching experiments, using a salt that remains in solution, provide a clear evidence for drug entrapment within MM.

A further and complementary approach to investigate the influence of incorporation inside MM on the lifetimes of excited states and the accessibility to ionic quenchers was based on LFP experiments, again in solution and in MM. Thus, the transient absorption spectra of NPX, CIN, and PPN in solution

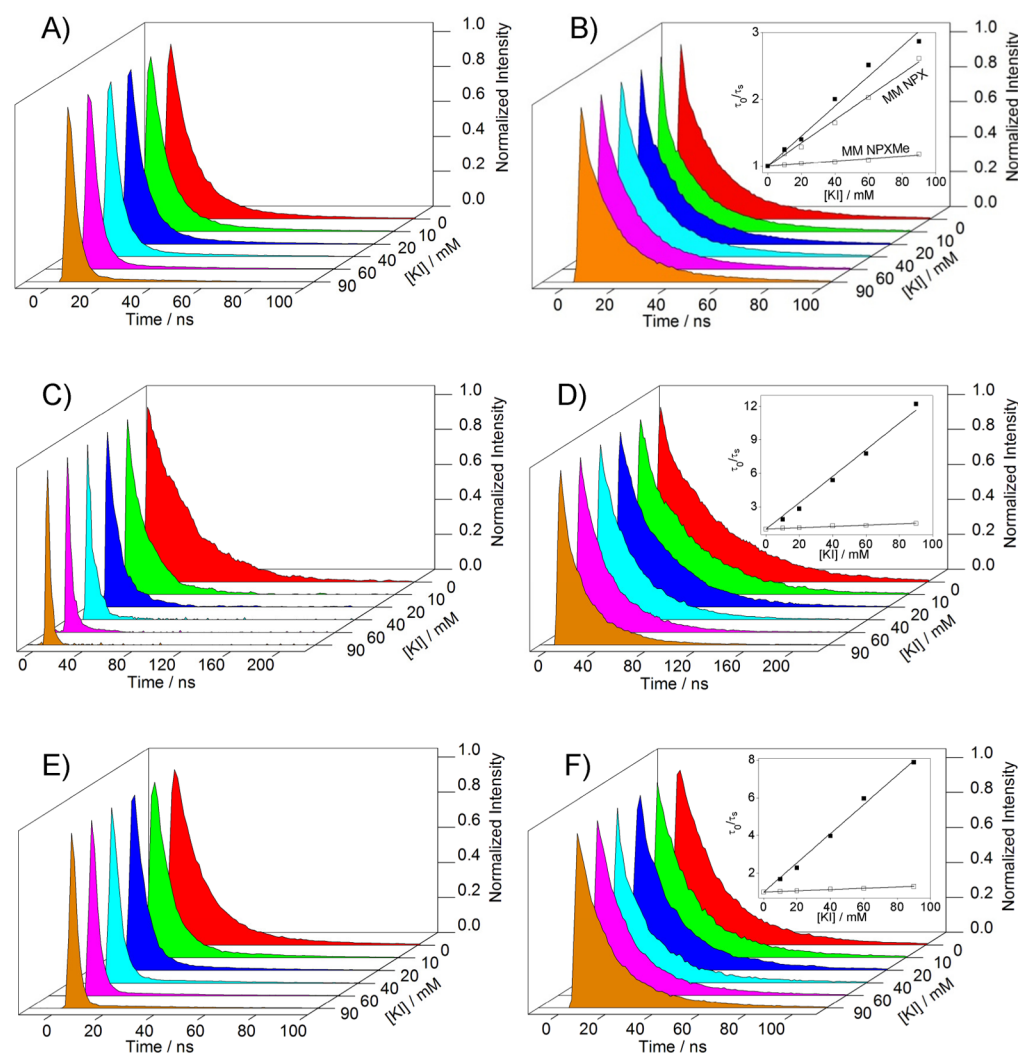


Figure 3. Changes in the emission decay traces ($\lambda_{\text{exc}} = 290$ nm) in the presence of increasing amounts of KI (0–90 mM) of NPX in 0.2 M aqueous NaCl (A) and its prodrug NPXMe into MM (B), CIN in 0.2 M aqueous NaCl (C) and into MM (D), PPN in 0.2 M aqueous NaCl (E) and into MM (F). Insets: Stern–Volmer plots in solution (■) and into MM (□).

Table 1. Rate Constants for Singlet Quenching by Iodide

drug	$k_{q,\text{sol}} \times 10^{-9} \text{ (M}^{-1}\cdot\text{s}^{-1})^{a,b}$	$k_{q,\text{MM}} \times 10^{-9} \text{ (M}^{-1}\cdot\text{s}^{-1})^a$
NPX	$2.70 \pm 0.13 \text{ (} 2.71 \pm 0.13 \text{)}$	$1.73 \pm 0.05 \text{ (} 1.53 \pm 0.03 \text{)}$
NPXMe		$0.15 \pm 0.01 \text{ (} 0.17 \pm 0.01 \text{)}$
CIN	$4.12 \pm 0.18 \text{ (} 3.59 \pm 0.07 \text{)}$	$0.22 \pm 0.01 \text{ (} 0.20 \pm 0.01 \text{)}$
PPN	$7.90 \pm 0.17 \text{ (} 6.95 \pm 0.05 \text{)}$	$0.24 \pm 0.01 \text{ (} 0.27 \pm 0.01 \text{)}$

^aThe experiments were performed three times, and the errors correspond to average deviations. ^bValues obtained from the steady-state measurements are given in parentheses.

displayed the typical naphthalene-like triplet–triplet absorption band^{27,28} at ca. 440 nm that remained unchanged upon incorporation into MM (Figure 4). However, a remarkable enhancement of the triplet lifetimes was observed for NPXMe, CIN, and PPN into MM, indicating the sensitivity of this excited state to the microenvironment (Figure 4).^{30,31} In fact, when quenching experiments were carried out in the presence of increasing concentrations of NaNO_2 , a small but significant quenching was observed in all cases, confirming the limited accessibility of the chromophores in the interior of MM. The triplet decays were fitted to a monoexponential function, and the quenching rate constants were determined in solution

($k_{q,\text{sol}}$) and in MM ($k_{q,\text{MM}}$) (Figure 4 insets and Table 2). Again a reduction by 1 order of magnitude was observed for NPXMe, CIN, and PPN upon incorporation into MM. Again, this effect was less pronounced in the case of NPX, indicating a higher accessibility to the quencher. For NPXMe and CIN the quenching plots were linear, whereas for PPN they were slightly curved. Thus, the data for PPN were also analyzed taking into account the in–out equilibrium, using the model previously described in the literature.³² Applying the above model, the rate constant determined for PPN triplet quenching by nitrite was $(1.32 \pm 0.04) \times 10^8 \text{ M}^{-1}\cdot\text{s}^{-1}$.

The obtained results are in complete agreement with those found from the fluorescence quenching experiments. Therefore, the LFP technique has demonstrated to be a very convenient tool to evaluate the influence of drugs entrapment within the MM microenvironment on the photophysical properties.

In summary, the singlet and triplet excited states of NPXMe, CIN, and PPN reveal efficient encapsulation of these drugs into MM. These species have proven to be useful reporters to evaluate the protection of chromophores from reagents that mainly remain in water. Moreover, a remarkable increase in the triplet lifetimes is also observed into MM, indicating the special environment existing in the interior of these microheteroge-

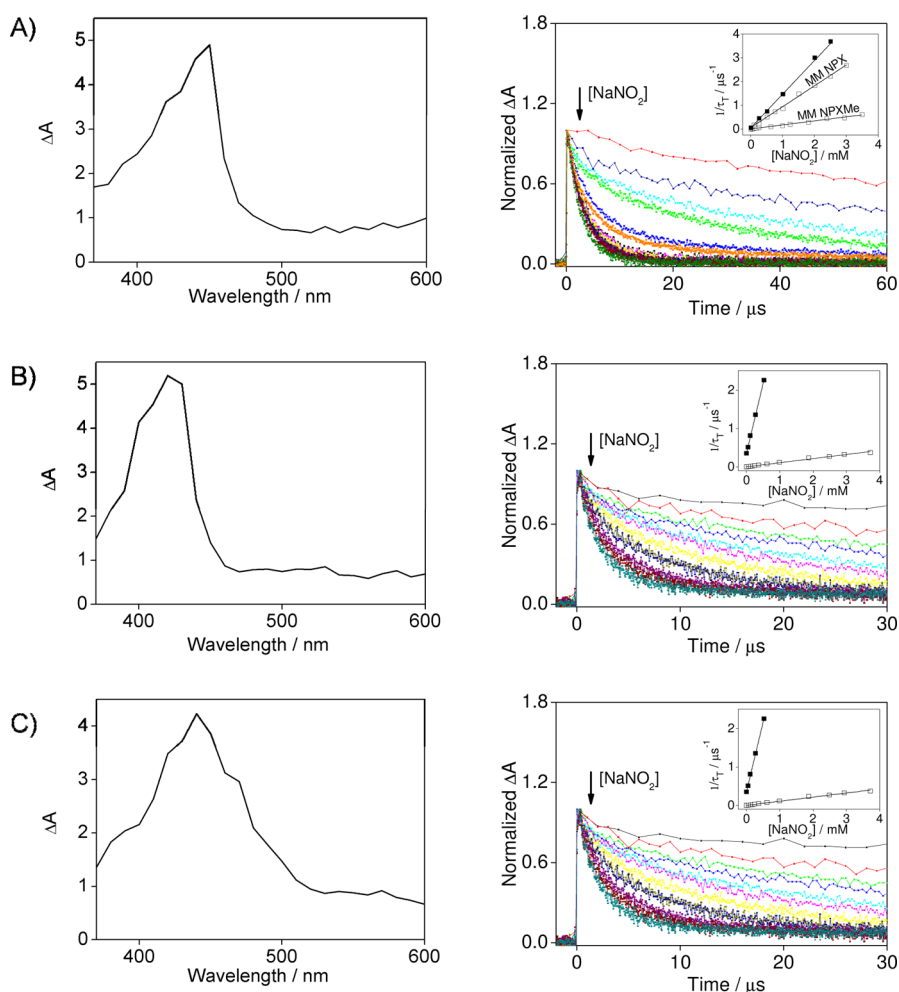


Figure 4. Transient absorption spectra (left) and decay traces (right) monitored at 420 nm ($\lambda_{\text{exc}} = 266$ nm) for drugs within MM in deaerated 0.2 M NaCl aqueous solution upon addition of increasing amounts of NaNO_2 : NPX(Me) (A), CIN (B), and PPN (C). Insets: Stern–Volmer plots in solution (■) and in the presence of MM (□).

Table 2. Determined Rate Constants for Triplet Quenching by Nitrite

drug	$k_{q,\text{sol}} \times 10^{-9} \text{ (M}^{-1}\cdot\text{s}^{-1})^a$	$k_{q,\text{MM}} \times 10^{-9} \text{ (M}^{-1}\cdot\text{s}^{-1})^a$
NPX	1.40 ± 0.03	0.88 ± 0.01
NPXMe ^b		0.17 ± 0.01
CIN	3.90 ± 0.10	0.11 ± 0.01
PPN	1.90 ± 0.07	0.18 ± 0.01^c

^aThe experiments were performed three times, and the errors correspond to average deviations. ^bFor solubility reasons the k_q for NPXMe triplet state was not determined in aqueous medium. ^cQuenching plots were slightly curved.

neous systems. Overall the combined fluorescence and LFP results demonstrate that photophysical techniques are non-invasive, direct, and valuable tools to assess how the encapsulation inside MM influences the excited state dynamics and accessibility to ionic quenchers. This approach can be in principle extended to other microheterogeneous systems capable of incorporating photoactive compounds.

AUTHOR INFORMATION

Corresponding Author

*E-mail address: mmiranda@qim.upv.es.

Notes

The authors declare no competing financial interest.

ACKNOWLEDGMENTS

Financial support from the Generalitat Valenciana (Prometeo Program), the Spanish Government (Red RETICS de Investigación de Reacciones Adversas a Alergenos y Fármacos (RIRAAF), Servet Contract CP11/00154 for I.A., CTQ2009-13699, CTQ2010-14882, CTQ2012-38754-C03-03 and Pre-doctoral FPU fellowship AP2008-03295 for M.G.-M.) is gratefully acknowledged.

REFERENCES

- (1) De Guidi, G.; Ragusa, S.; Cambria, M. T.; Belvedere, A.; Catalfo, A.; Cambria, A. Photosensitizing Effect of Some Nonsteroidal Antiinflammatory Drugs on Natural and Artificial Membranes: Dependence on Phospholipid Composition. *Chem. Res. Toxicol.* **2005**, *18*, 204–212.
- (2) Iglesias, E. Exploring the Effect of Supramolecular Structures of Micelles and Cyclodextrins on Fluorescence Emission of Local Anesthetics. *Photochem. Photobiol. Sci.* **2011**, *10*, 531–542.
- (3) Jimenez, M. C.; Miranda, M. A.; Tormos, R. Photochemistry of Naproxen in the Presence of β -Cyclodextrin. *J. Photochem. Photobiol., A* **1997**, *104*, 119–121.
- (4) Sortino, S. Selective Entrapment of the Cationic Form of Norfloxacin Within Anionic Sodium Dodecyl Sulfate Micelles at

Physiological pH and its Effect on the Drug Photodecomposition. *Photochem. Photobiol.* **2006**, *82*, 64–70.

(5) Hammad, M. A.; Muller, B. W. Increasing Drug Solubility by Means of Bile Salt-Phosphatidylcholine-Based Mixed Micelles. *Eur. J. Pharm. Biopharm.* **1998**, *46*, 361–367.

(6) Porter, C. J. H.; Charman, W. N. In Vitro Assessment of Oral Lipid Based Formulations. *Adv. Drug Delivery Rev.* **2001**, *50*, S127–S147.

(7) Porter, C. J. H.; Trevaskis, N. L.; Charman, W. N. Lipids and Lipid-Based Formulations: Optimizing the Oral Delivery of Lipophilic Drugs. *Nat. Rev. Drug Discovery* **2007**, *6*, 231–248.

(8) Rangel-Yagui, C. O.; Pessoa, A.; Tavares, L. C. Micellar Solubilization of Drugs. *J. Pharm. Pharmacol. Sci.* **2005**, *8*, 147–163.

(9) Garidel, P. L.; Mixed, J. Vesicles and Mixed Micelles: Formation, Thermodynamic Stability, and Pharmaceutical Aspects. In *Liposome Technology*, 3rd ed.; Informa Healthcare USA: New York, 2006; Vol. 1, pp 209–239.

(10) Hammad, M. A.; Muller, B. W. Solubility and Stability of Tetracepam in Mixed Micelles. *Eur. J. Pharm. Sci.* **1998**, *7*, 49–55.

(11) Hammad, M. A.; Muller, B. W. Solubility and Stability of Clonazepam in Mixed Micelles. *Int. J. Pharm.* **1998**, *169*, 55–64.

(12) Hendradi, E.; Obata, Y.; Isowa, K.; Nagai, T.; Takayama, K. Effect of Mixed Micelle Formulations Including Terpenes on the Transdermal Delivery of Diclofenac. *Biol. Pharm. Bull.* **2003**, *26*, 1739–1743.

(13) Parsaee, S.; Sarbolouki, M. N.; Parnianpour, M. In-Vitro Release of Diclofenac Diethylammonium from Lipid-Based Formulations. *Int. J. Pharm.* **2002**, *241*, 185–190.

(14) Hammad, M. A.; Muller, B. W. Factors Affecting Solubility and Stability of Indomethacin in Mixed Micelles. *Pharmazie* **1998**, *53*, 790–794.

(15) Song, X.; Jiang, Y.; Ren, C.; Sun, X.; Zhang, Q.; Gong, T.; Zhang, Z. Nimodipine-Loaded Mixed Micelles: Formulation, Compatibility, Pharmacokinetics, and Vascular Irritability Study. *Int. J. Nanomed.* **2012**, *7*, 3689–3699.

(16) Yu, J.-n.; Zhu, Y.; Wang, L.; Peng, M.; Tong, S.-s.; Cao, X.; Qiu, H.; Xu, X. M. Enhancement of Oral Bioavailability of the Poorly Water-Soluble Drug Silybin by Sodium Cholate/Phospholipid-Mixed Micelles. *Acta Pharmacol. Sin.* **2010**, *31*, 759–764.

(17) Sznitowska, M.; Klunder, M.; Placzek, M. Paclitaxel Solubility in Aqueous Dispersions and Mixed Micellar Solutions of Lecithin. *Chem. Pharm. Bull.* **2008**, *56*, 70–74.

(18) Alkanonyuksel, H.; Ramakrishnan, S.; Chai, H. B.; Pezzuto, J. M. A Mixed Micellar Formulation Suitable for the Parenteral Administration of Taxol. *Pharm. Res.* **1994**, *11*, 206–212.

(19) Cohen, D. E.; Thurston, G. M.; Chamberlin, R. A.; Benedek, G. B.; Carey, M. C. Laser Light Scattering Evidence for a Common Wormlike Growth Structure of Mixed Micelles in Bile Salt- and Straight-Chain Detergent-Phosphatidylcholine Aqueous Systems: Relevance to the Micellar Structure of Bile. *Biochemistry* **1998**, *37*, 14798–14814.

(20) Sun, C. Q.; Sano, Y.; Kashiwagi, H.; Ueno, M. Characterization of Aggregate Structures of Phospholipid in the Process of Vesicle Solubilization with Sodium Cholate Using Laser Light Scattering Method. *Colloid Polym. Sci.* **2002**, *280*, 900–907.

(21) de la Maza, A.; Manich, A. M.; Parra, J. L. Intermediate Aggregates Resulting in the Interaction of Bile Salt With Liposomes Studied by Transmission Electron Microscopy and Light Scattering Techniques. *J. Microsc.-Oxford* **1997**, *186*, 75–83.

(22) Schwarz, M. A.; Raith, K.; Ruettinger, H. H.; Dongowski, G.; Neubert, R. H. H. Investigation of the Interactions Between Drugs and Mixed Bile Salt/Lecithin Micelles. A Characterization by Micellar Affinity Capillary Electrophoresis (MACE). Part III. *J. Chromatogr., A* **1997**, *781*, 377–389.

(23) Hildebrand, A.; Neubert, R.; Garidel, P.; Blume, A. Bile Salt Induced Solubilization of Synthetic Phosphatidylcholine Vesicles Studied by Isothermal Titration Calorimetry. *Langmuir* **2002**, *18*, 2836–2847.

(24) Muller, K. Structural Dimorphism of Bile Salt/Lecithin Mixed Micelles. A Possible Regulatory Mechanism for Cholesterol Solubility in Bile? X-Ray Structure Analysis. *Biochemistry* **1981**, *20*, 404–14.

(25) Yuet, P. K.; Blankschtein, D.; Donovan, J. M. Ultracentrifugation Systematically Overestimates Vesicular Cholesterol Levels in Bile. *Hepatology* **1996**, *23*, 896–903.

(26) Stark, R. E.; Roberts, M. F. 500 MHz Proton NMR Studies of Bile Salt-Phosphatidylcholine Mixed Micelles and Vesicles. Evidence for Differential Motional Restraint on Bile Salt and Phosphatidylcholine Resonances. *Biochim. Biophys. Acta—Biomembr.* **1984**, *770*, 115–21.

(27) Gomez-Mendoza, M.; Nuin, E.; Andreu, I.; Marin, M. L.; Miranda, M. A. Photophysical Probes to Assess the Potential of Cholic Acid Aggregates as Drug Carriers. *J. Phys. Chem. B* **2012**, *116*, 10213–10218.

(28) Nuin, E.; Gomez-Mendoza, M.; Andreu, I.; Marin, M. L.; Miranda, M. A. New Photoactive Compounds to Probe Cholic Acid and Cholesterol inside Mixed Micelles. *Org. Lett.* **2013**, *15*, 298–301.

(29) Tsai, S. W.; Huang, C. M. Enantioselective Synthesis of (S)-Suprofen Ester Prodrugs by Lipase in Cyclohexane. *Enzyme Microb. Technol.* **1999**, *25*, 682–688.

(30) Nuin, E.; Andreu, I.; Torres, M. J.; Jimenez, M. C.; Miranda, M. A. Enhanced Photosafety of Cinacalcet upon Complexation with Serum Albumin. *J. Phys. Chem. B* **2011**, *115*, 1158–1164.

(31) Perez-Ruiz, R.; Alonso, R.; Nuin, E.; Andreu, I.; Jimenez, M. C.; Miranda, M. A. Naphthalene Triplet Excited State as a Probe for the Assessment of Drug Distribution in Binary Protein Systems. *J. Phys. Chem. B* **2011**, *115*, 4460–4468.

(32) Bohne, C. Supramolecular Dynamics Studied Using Photo-physics. *Langmuir* **2006**, *22*, 9100–9111.